

Zdzisław GOSIEWSKI, Marcin SZARO
WOJSKOWA AKADEMIA TECHNICZNA, WYDZIAŁ MECHATRONIKI

Actuator/Sensor Integration in Magnetic Bearings

Prof. dr hab. inż. Zdzisław Gosiewski

Profesor zwyczajny na Wydziale Mechatroniki, Wojskowej Akademii Technicznej. Ukończył Politechnikę Gdańską w 1974 r. Karierę naukową od asystenta stażysty do profesora nadzwyczajnego realizował na Politechnice Koszalińskiej. Zajmuje się mechatroniką stosowaną, a szczególnie sterowaniem drganiami maszyn wirnikowych z wykorzystaniem łożysk magnetycznych, oraz nawigacją i sterowaniem statków powietrznych. Autor i współautor 5 monografii, 1 skryptu, oraz ok. 150 artykułów i referatów. Wypromował 5 doktorów nauk technicznych.



gosiewski@wmt.wat.edu.pl

Mgr inż. Marcin Szaro

Jest asystentem na Wydziale Mechatroniki, Wojskowej Akademii Technicznej. Ukończył WAT w 1997r. Główne zainteresowania naukowe dotyczą miernictwa, awioniki i diagnostyki. Te dziedziny wykorzystuje w przygotowywanej rozprawie doktorskiej.



szaro@wmt.wat.edu.pl

Streszczenie

W artykule omówiono możliwość wykorzystania cewki elektromagnesu łożysk magnetycznych jako elementu pomiarowego. Przedstawiona została matematyczna analiza zjawisk fizycznych zachodzących w obwodzie czujnika indukcyjnościowego. Model ten został zaimplementowany w środowisku Matlab, a przykładowe charakterystyki obwodu pomiarowego czujnika przedstawione są w artykule. Opisane zostały również charakterystyki statyczne i dynamiczne układu pomiarowego uzyskane na stanowisku laboratoryjnym.

Abstract

In this paper we consider sensor and actuator integration in a magnetic bearing. The mathematical analysis of physical effects in a inductive sensor circuit is carried out. This model is implemented in the software environment of Matlab. There are shown simulation characteristics of measurement circuit of sensor. We present experimental static and dynamics characteristics, particularly static linear characteristics and step responses obtained on a prototype lab stand. We indicate the future directions of research of inductive sensor in suggested system.

Keywords: displacement sensor, magnetic bearing, synergy, reliability

1. Introduction

Eddy currents sensors are usually applied in magnetic bearings for non-contact measurement of rotor displacements. They have disadvantages:

- they are relatively expensive - the cost of eddy current sensors is significant part of magnetic bearing price;
- the calculation of offset is required;
- usually they are not collocated with actuator.

For these reasons, we are looking for other solutions of rotor displacement measurement. In the paper we propose an inductive sensor with a high frequency RLC resonant circuit with coils of magnetic bearings as a part of measuring components. It leads to the collocation of sensors and actuators and reduces the number of sensor/actuator components. Finally, the system reliability increases. Such approach was considered in [1]. We extended those results to use the classical control circuit with analog amplifiers.

The high frequency circuit of the measurement system is separated from the low frequency magnetic bearing control system. For measurement proposes an external capacitor is added to one of serially joined coils in each of the magnetic bearing axes. Voltage from the capacitor is demodulated. Signal value depends only on dislocation of rotor from neutral (magnetic bearing centre) position. In the paper, we describe mathematical model of measurement system. The model was simulated in Matlab-Simulink environment.

A prototype of measurement system was tested on the lab stand with full magnetic levitation system of rigid rotor (Fig. 1). There are two radial and one axial magnetic bearings. Stator of radial

bearing consists of eight coils (four for each controlled axis). Coils are connected in such a way that their fluxes sum up. We have fixed two rings on the rotor. The first one is made as an electromagnet path. It's build from siliceous sheets. The second one is an aluminium sleeve which interacts with eddy currents sensor.

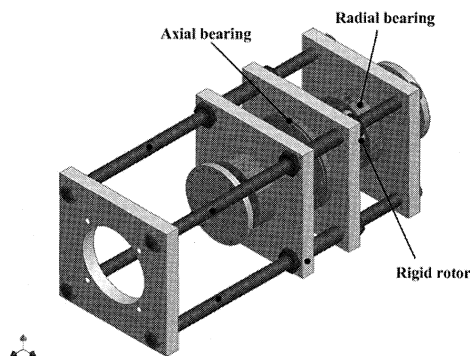


Fig. 1. Lab stand for testing of rigid rotors with magnetic bearings

2. Measurement System

Proposed solution of inductive sensor utilizes two opposite coils of magnetic bearing (Fig. 2). Let x is a distance of the shaft surface from pole of the electromagnet. Omitting a dispersed flux, we can write the equation for self-inductance L for one-side electromagnetic coils as follows [2]:

$$L(x) = \frac{z^2}{R_{\mu Fe} + R_{\mu p}} = \frac{z^2}{\frac{l_{Fe}}{\mu_{Fe} A_{Fe}} + \frac{2x}{\mu_p A_p}} \quad (1)$$

where:

- z - number of coils; R_{μ} - magnetic reluctance;
- x - distance between rotor and electromagnet core;
- l_{Fe} - length of core;
- μ_{Fe} - permeability of steel; $\mu_p \approx \mu_0$ - air permeability;
- A_p, A_{Fe} - cross-section of air and steel core, respectively.

As we can see, the self-inductance described by equation (1) is a nonlinear function of the distance x . Impedance is a nonlinear function of air-gap x , too. To linearize the characteristic (1) in the operation point (usually, in the centre of magnetic bearing) we are using two opposite electromagnetic coils (see Fig. 2) in the differential serial configuration.

An external capacitor is added to one of serial joined coils in each of controlled axes of magnetic bearing. Thus, we have a complex resonant circuit as it is seen in the Fig. 3. The supply voltage (U_{supply}) is a sum of two signals. The first one is a control signal supplying the bearing actuator, and the second one is a high frequency supply of the sensor.

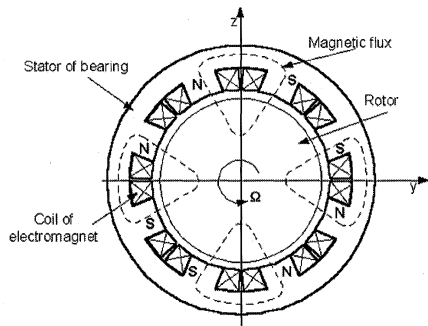


Fig. 2. Components of heteropolar actuator of magnetic bearing used as sensor components

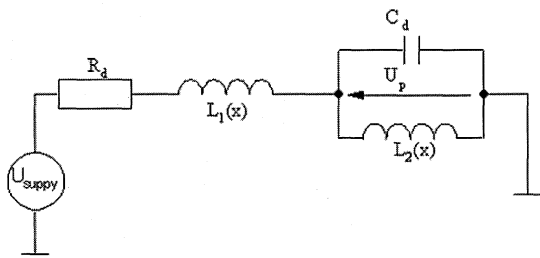


Fig. 3. Diagram of resonant sensor circuit

The voltage measured on the capacitor is the modulating signal. The frequency of the supply voltage is the carrier frequency while the displacement signal is the modulated signal. The demodulation process consists of a few steps (Fig. 4). The absolute value of output voltage (Fig. 3) is determined in the first step. In the next, we average the absolute value through low-pass filtering. Such signal is a nonlinear function of measured displacement. To linearize displacement signal we connect two filtered signals from opposite coils (in one measurement axis) in differential way.

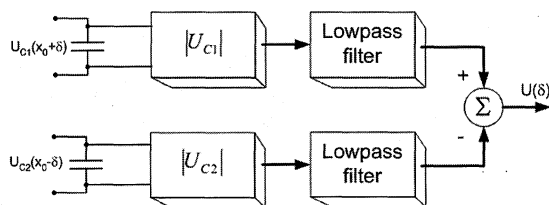


Fig. 4. Scheme of signal processing

2.1 Simulation results

The impedance of complete circuit (Fig. 3) is given by equation:

$$Z = R_d + j \left(\omega L_1(x) - \frac{\omega L_2(x)}{\omega^2 L_2(x) C_d - 1} \right) \quad (2)$$

where:

R_d - substitute resistance of circuit; C_d - additional capacitance.
 $x = x_0 \pm \delta$.

We can describe current in the circuit by relation: $I = U_{supply}/Z$. Voltage on the external capacitor is a measured signal. The modulus of the voltage is given by the following equation:

$$U_p = I \cdot \left(\frac{\omega L_2(x)}{\omega^2 L_2(x) C_d - 1} \right) \quad (3)$$

The frequency of supply voltage (see Fig. 5) should be selected in such a way that it is higher than a frequency of the resonant peak for maximal measurement displacement ($f_{supply} > f_{o|x_{max}}$). This is necessary condition to make the measurement signal unique.

Sensor designed according to Fig. 4 has got different characteristics in comparison to simulated ones (Fig. 5) of circuit diagram from Fig. 3. To approach the real characteristics observed on oscilloscope we have designed a new equivalent circuit scheme shown in Fig. 6.

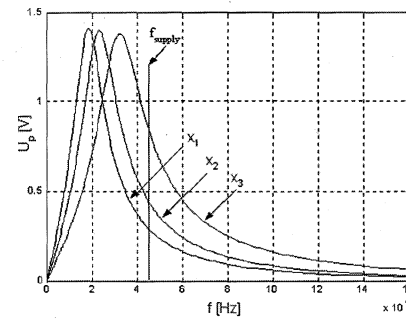


Fig. 5. The output voltage as function of frequency for different air-gap $x_3 > x_2 > x_1$

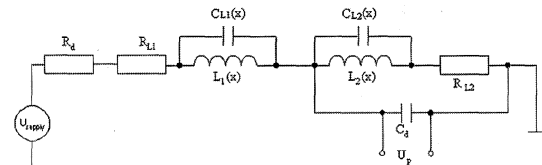


Fig. 6. Circuit scheme with parasitic capacitance

The admittance of circuit from Fig. 6 is described by the following relation:

$$Y_1 = \omega C_L - \frac{1}{\omega L} \Rightarrow \frac{1}{Y_1} = \frac{1}{\omega C_L - \frac{1}{\omega L}} = \frac{\omega L}{\omega^2 LC_L - 1} \quad (4)$$

where:

$L = L_1 + M_{21} = L_2 + M_{12}$ and M_{12}, M_{21} - mutual inductances;
 C_{L1}, C_{L2} - parasitic capacitance of coils.

When we take into account the resistance of coil we have:

$$Z_1 = R + j \frac{1}{Y_1} = R - j \frac{\omega L}{\omega^2 LC_L - 1} \quad (5)$$

where: $R = R_{L1} = R_{L2}$ - resistance of coils.

The coil impedance with the additional capacitance is given by: (6)

$$Z_2 = \frac{R}{\left(1 + \frac{\omega^2 LC_d}{\omega^2 LC_L - 1}\right)^2 + \omega^2 R^2 C_d^2} - j \frac{\left(1 + \frac{\omega^2 LC_d}{\omega^2 LC_L - 1}\right) \cdot \frac{\omega L}{\omega^2 LC_L - 1} + \omega R^2 C_d}{\left(1 + \frac{\omega^2 LC_d}{\omega^2 LC_L - 1}\right)^2 + \omega^2 R^2 C_d^2}$$

The impedance of complete circuit from Fig. 6 is given by equation (7):

$$Z_w = R_d + Z_1 + Z_2 = R_d + R + \frac{R}{\left(1 + \frac{\omega^2 LC_d}{\omega^2 LC_L - 1}\right)^2 + \omega^2 R^2 C_d^2} -$$

$$j \frac{\left(1 + \frac{\omega^2 LC_d}{\omega^2 LC_L - 1}\right) \cdot \frac{\omega L}{\omega^2 LC_L - 1} + \omega R^2 C_d}{\left(1 + \frac{\omega^2 LC_d}{\omega^2 LC_L - 1}\right)^2 + \omega^2 R^2 C_d^2}$$

Thus, the current modulus for this circuit is as follows: (8)

$$I = \frac{U_{supply}}{\sqrt{\left(R_d + R + \frac{R}{\left(1 + \frac{\omega^2 LC_d}{\omega^2 LC_L - 1}\right)^2 + \omega^2 R^2 C_d^2} \right)^2 + \left(\frac{\omega L}{\omega^2 LC_L - 1} \cdot \frac{\left(1 + \frac{\omega^2 LC_d}{\omega^2 LC_L - 1}\right) \cdot \frac{\omega L}{\omega^2 LC_L - 1} + \omega R^2 C_d}{\left(1 + \frac{\omega^2 LC_d}{\omega^2 LC_L - 1}\right)^2 + \omega^2 R^2 C_d^2} \right)^2}}$$

The modulus (amplitude) of measurement voltage is defined as: (9)

$$U_p = I \cdot \sqrt{\left(\frac{R}{\left(1 + \frac{\omega^2 LC_d}{\omega^2 LC_L - 1}\right)^2 + \omega^2 R^2 C_d^2} \right)^2 + \left(\frac{\left(1 + \frac{\omega^2 LC_d}{\omega^2 LC_L - 1}\right) \cdot \frac{\omega L}{\omega^2 LC_L - 1} + \omega R^2 C_d}{\left(1 + \frac{\omega^2 LC_d}{\omega^2 LC_L - 1}\right)^2 + \omega^2 R^2 C_d^2} \right)^2}}$$

It leads to the amplitude-frequency characteristic typical for resonant circuits connected serially (Fig. 7) for the case of constant amplitude of AC supply voltage. In comparison with Fig. 5 we can see that resonant peaks are situated in different places (the other frequencies) and they values are different for the same displacements.

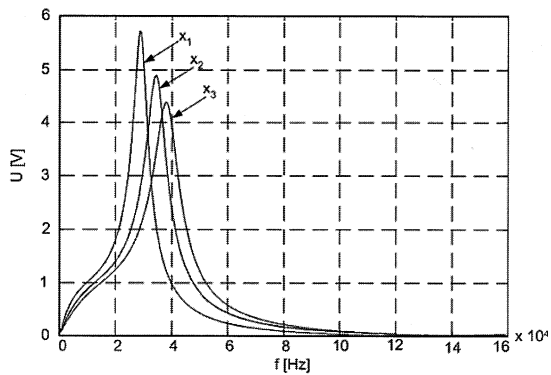


Fig. 7. The output voltage signal of the circuit from Fig. 4 as function of frequency for air-gaps: $x_3 > x_2 > x_1$

2.2 Experimental results

In the next step, the verification of simulation model in a lab stand was made. At first, we measured static characteristics. The output signals from model of sensor was compared with eddy currents sensor. This characteristic is shown in Fig. 8. The characteristic is linear in whole range of displacement (in the vicinity of operation point). The characteristic of the inductive sensor has bigger slope. It indicates higher sensor resolution.

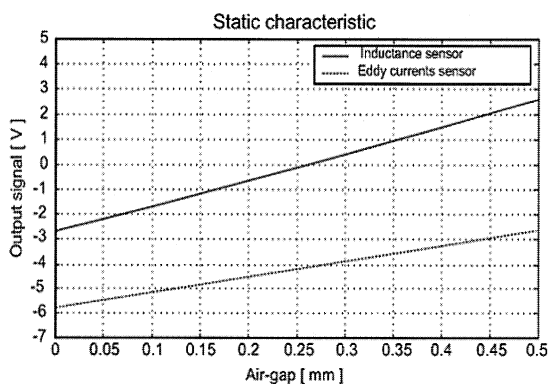


Fig. 8. Static characteristic for one measurement axis

In the second step of the investigation we obtained the step responses of rotor-exiter system. The examples of experimental step responses are presented in Fig. 9.

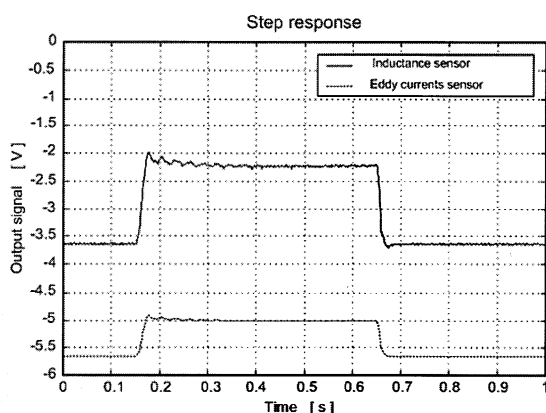


Fig. 9. Step response of rotor-exiter system

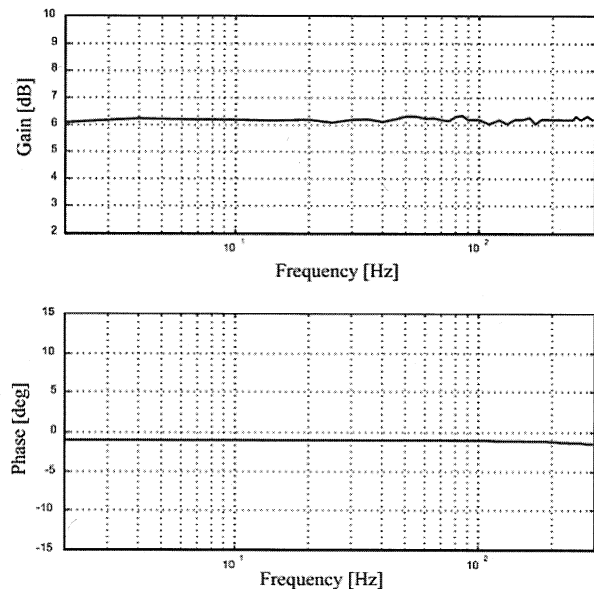


Fig. 10. Bode diagram of inductive sensor

Finally, we measured Bode diagram for frequency range 1 - 300 [Hz] (Fig. 10). To do that we used the electrodynamics exiter. Magnitude and phase of Bode diagram are straight lines in this range. Phase shift is about 1 [deg]. Due to limitation of exiter frequency range we could not register the Bode diagram in a wider range (displacement of rotor for frequency over 300 [Hz] was too small to measured).

3. Conclusions

As it was mentioned earlier, the resonant circuit should be designed to isolate the control and sensor voltage signals by wide separation the control and sensor frequencies. The control signal is a sum of many rectangular signals. Spectrum of control signal consists of many harmonics. The basic harmonic has the same frequency as the sampling frequency of control signal. So, we should choose frequency of control signal in such a way that harmonics do not disturb sensor supply signal (in the case when frequency of sensor supply signal is bigger than frequency of control signal). If the frequency of sensor supply signal is smaller than frequency of control signal, they have to be considerably different. In lab stand we use amplifiers with limited band, so in future research we have to use stand-alone DSP system to integrate the sensor and actuator circuits.

The RLC inductive sensor have got linear static characteristic in the vicinity of the magnetic bearing operation point. It has also high sensitivity similar to eddy currents sensor. The bandwidth depends on frequency of supply voltage. When we use high frequency, the bandwidth is higher, but we have to take into consideration similar like eddy currents sensor effects. In our model of inductive sensor we confirmed the linearity of the frequency band to 300 [Hz]. In future research we will work out a method of sensor auto-diagnostics.

References

- [1] Choi C., Park K.: A sensorless magnetic levitation system using a LC resonant circuit with PPF control, MOVIC'98, Zurich 1998, Volume 2, pp. 739-744.
- [2] Łapiński M.: Pomiary elektryczne i elektroniczne wielkości nieelektrycznych, Warszawa 1974, pp. 77-86.

Tytuł: Synergia elementu pomiarowego z wykonawczym w łożyskach magnetycznych

Artykuł recenzowany